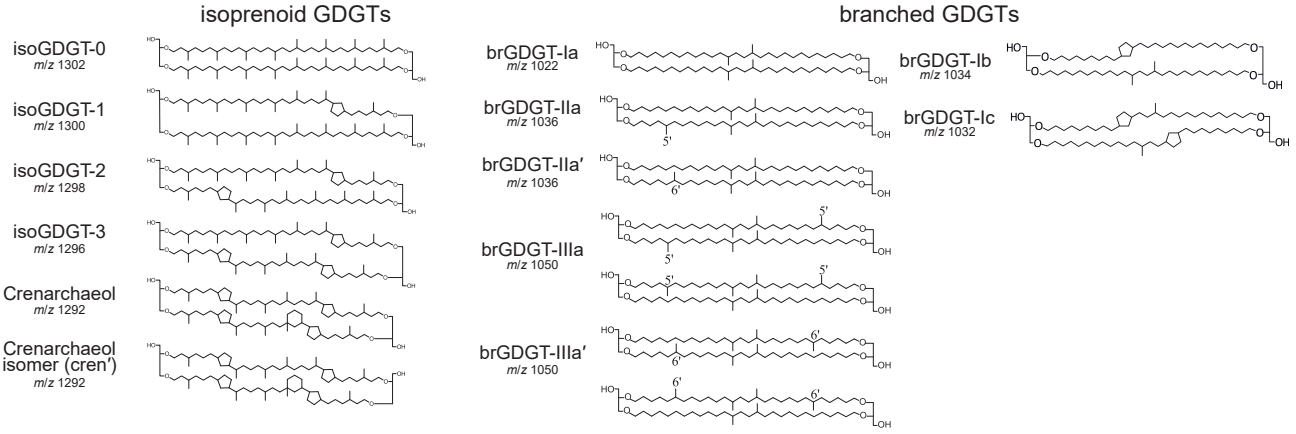

Figure S1. Molecular structure and names of iso- and brGDGTs used in the indices presented in this study. BrGDGTs with one (as in IIa and IIa′) and two (as in IIIa and IIIa′) additional methyl groups may also include one or two rings (i.e., IIb-c, IIb-c′, IIIb-c and IIIb-c′; structures not shown).

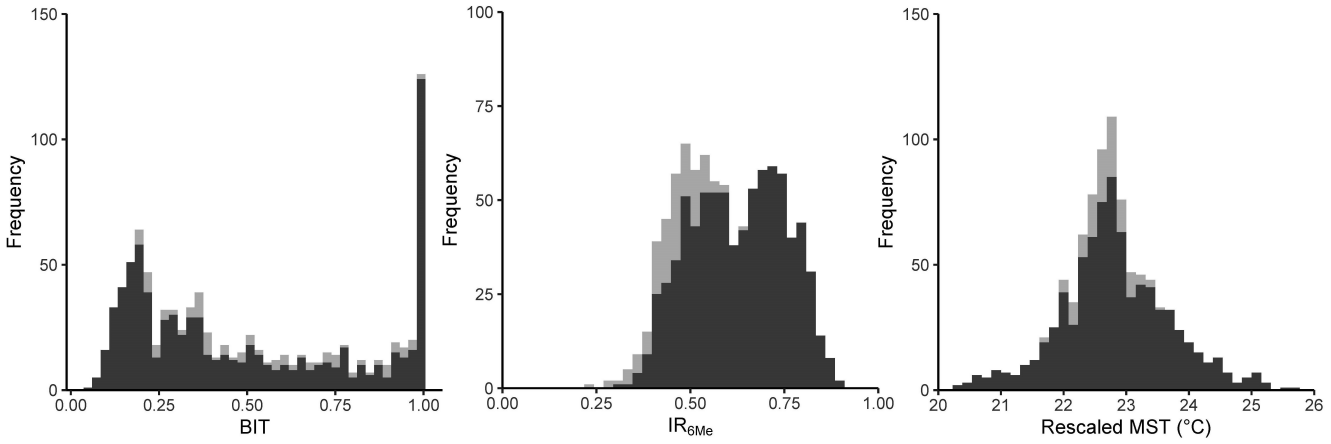

Figure S2. Distribution of calculated values for (a) the BIT index (b) $\mathrm{IR_{6Me}}$ and (c) rescaled MST (mean summer temperature; Pearson et al. (2011); Baxter et al. (2023)) throughout the full DeepCHALLA sequence (250 - 0 ka; light grey) and during the period 180 - 0 ka (dark grey).

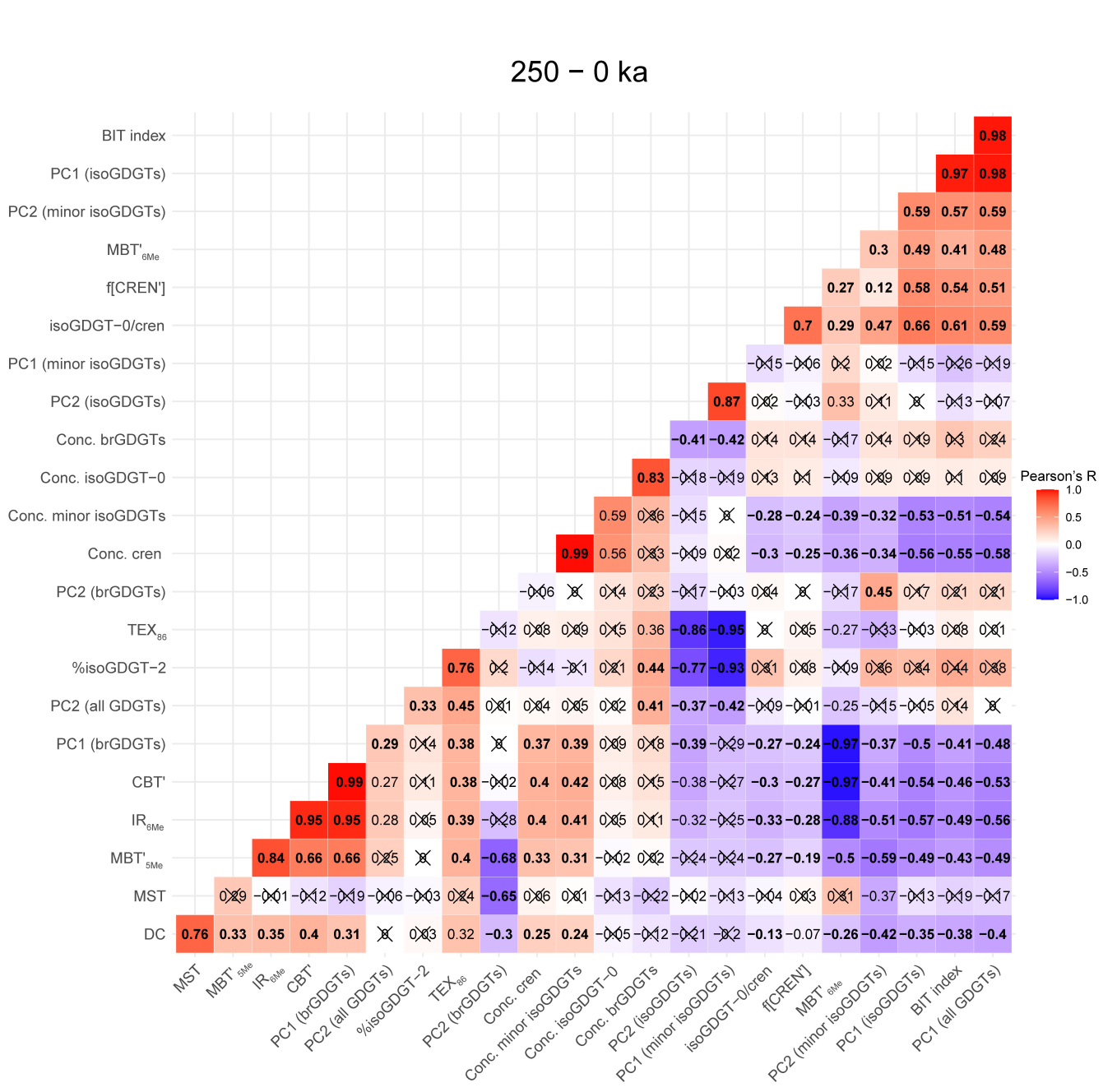

Figure S3. Correlation (pearson) matrix between GDGT concentration, indices, and principal component (PC) scores for the full DeepCHALLA sequence. Squares marked with x are not significantly correlated ($p > 0.01$). Correlation coefficients (R value) of significantly correlated variable are indicated with normal script used to reflect those cases where $p < 0.01$, and bold text for where $p < 0.001$.

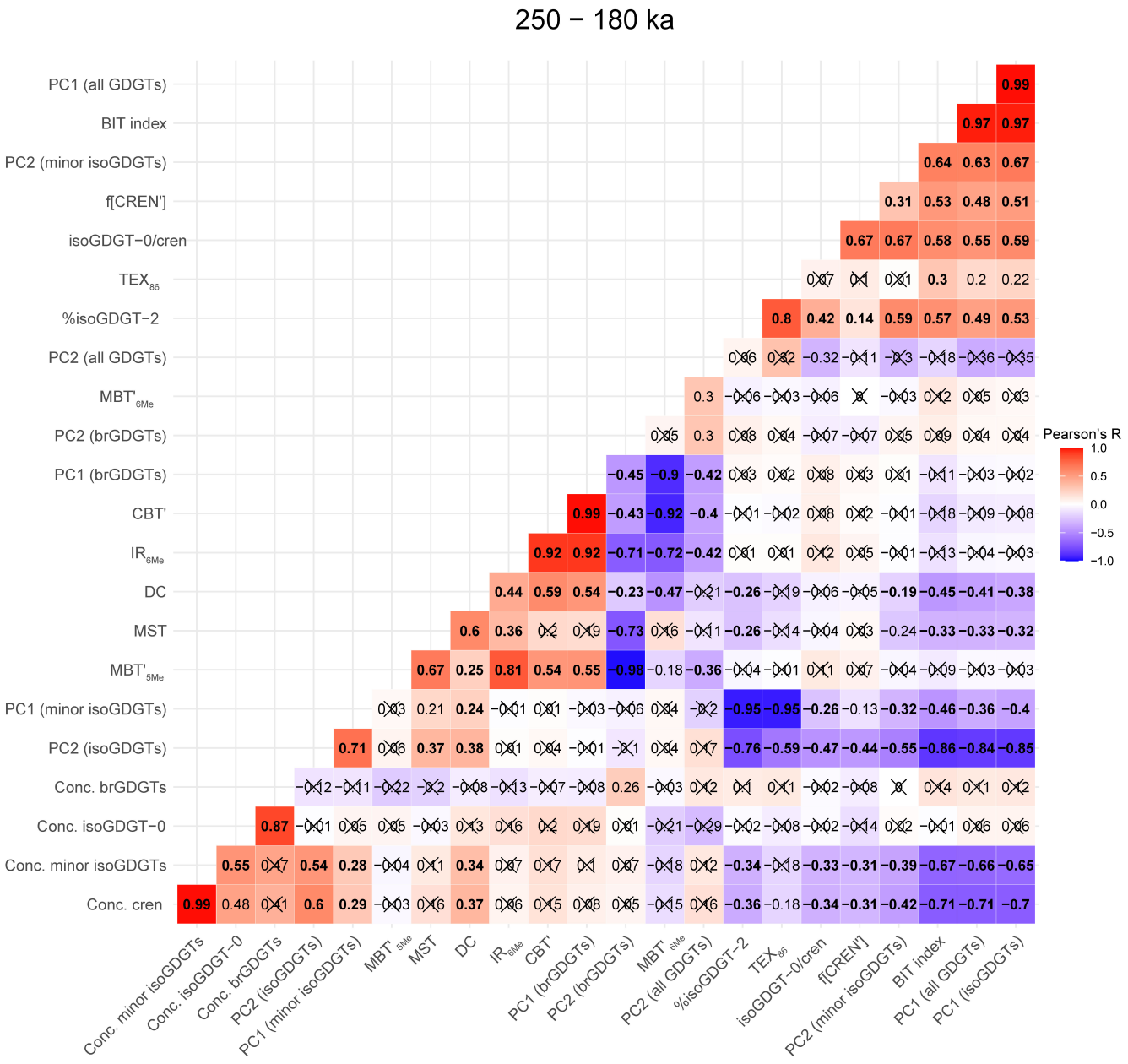

Figure S4. As described in Fig. S3 but for the period 250–180 ka of the DeepCHALLA sequence.

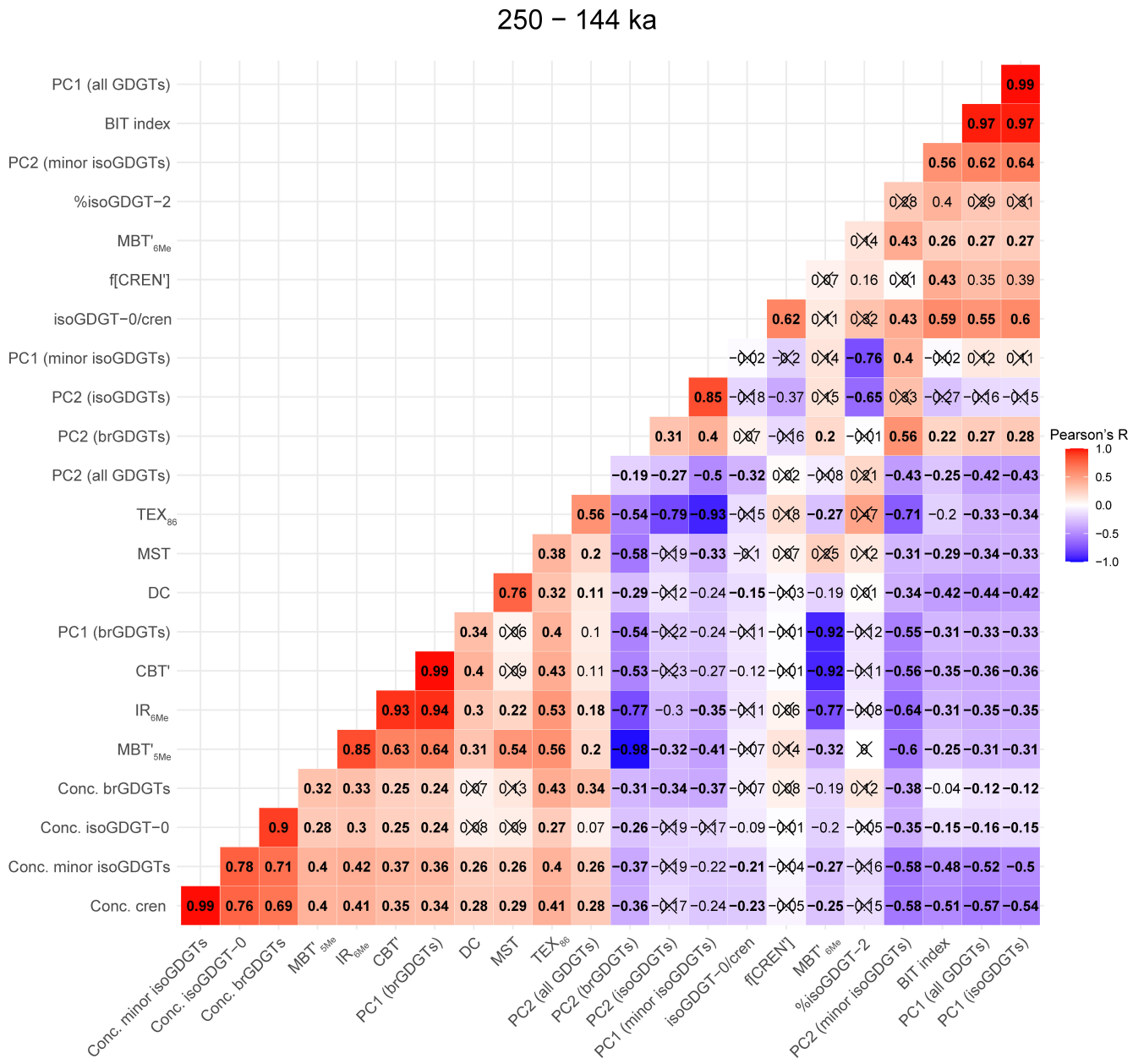

Figure S5. As described in Fig. S3 but for the period 250–144 ka of the DeepCHALLA sequence.

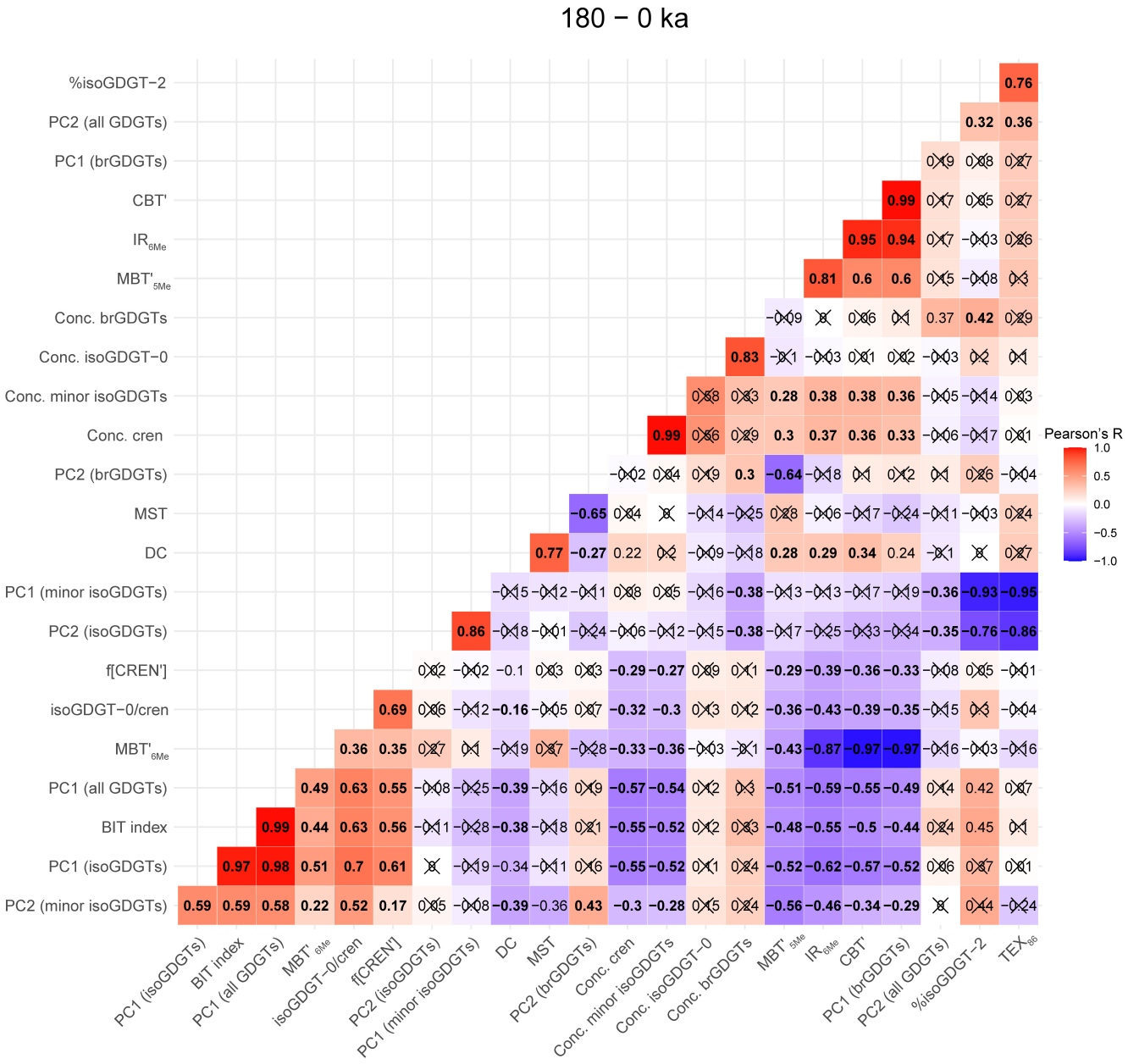

Figure S6. As described in Fig. S3 but for the period 180–0 ka of the DeepCHALLA sequence.

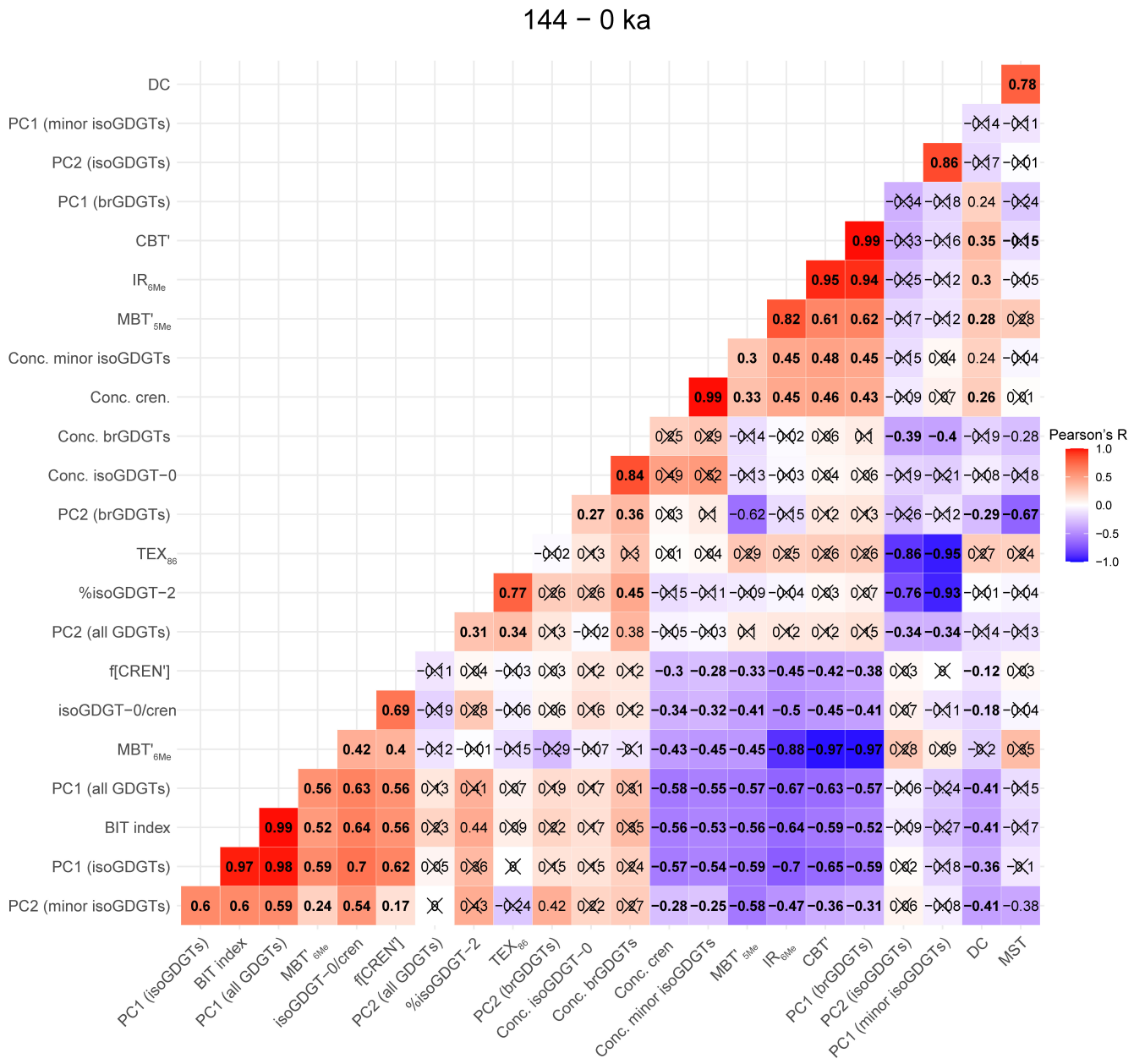

Figure S7. As described in Fig. S3 but for the period 144–0 ka of the DeepCHALLA sequence.

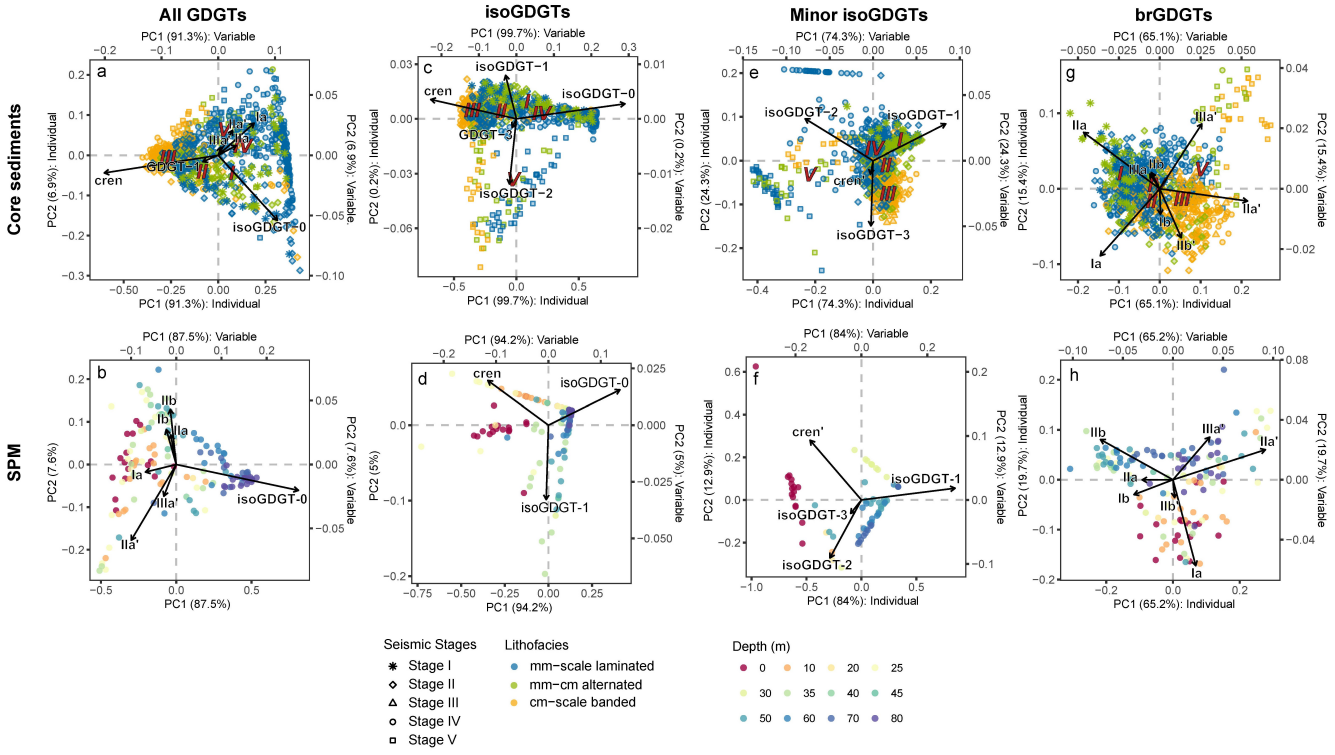

Figure S8. Principal component analysis of the fractional abundance of GDGTs in the DeepCHALLA core and suspended particulate matter (SPM). PCA of all GDGTs in (a) DeepCHALLA and in (b) the SPM, the isoGDGTs in (c) DeepCHALLA and (d) the SPM, the minor isoGDGTs (i.e., isoGDGT-1, -2, -3 and the crenarchaeol isomer) in (e) the DeepCHALLA sequence and (f) the SPM, and the brGDGTs in (g) DeepCHALLA and (h) the SPM. The loadings of GDGTs are shown in the plot with arrows. In cases where GDGTs contributed < 1% of the variability of the data on both PC1 and PC2 were removed to improve readability (but their fractional abundances were still included during analysis). Individual scores of DeepCHALLA sediment horizons (panels a, c, e, g) are colored according to lithofacies, with seismic stage indicate by different symbols. Red numerals (V-I) in panels (a, c, e, and g) represent the centroid values (i.e., average PC scores) of sequence separated according to the depositional stages. SPM in panels (b, d, f, and h) are colored according to sampling depth. Note that separate PC axes indicate the position of the individuals (sediment horizons) and variables (GDGT vectors) and that the amount of variability within the dataset predicted by PC1 and PC 2 is provided as a percentage (in brackets).

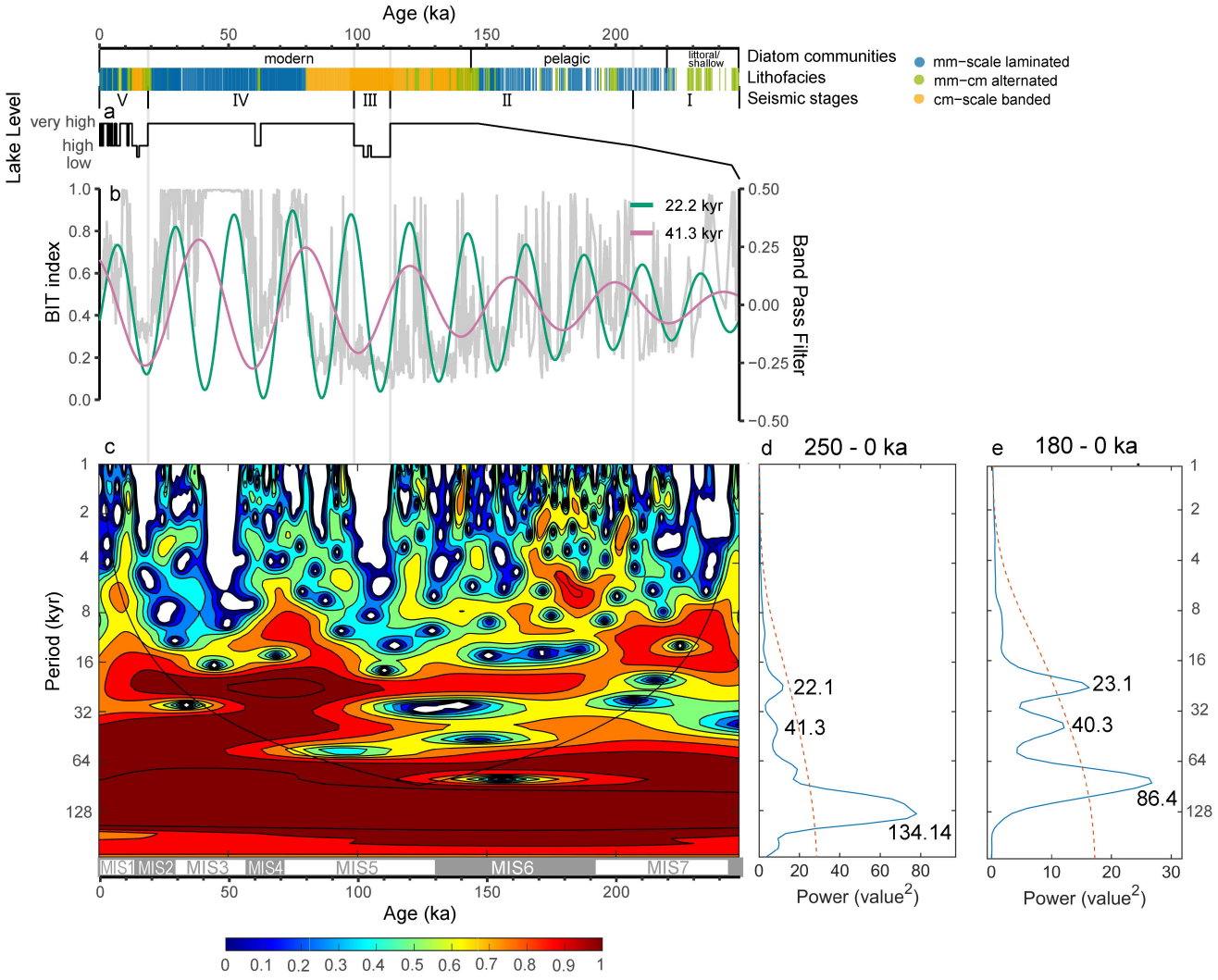

Figure S9. Periodicity analysis of the BIT index. Indicated from top to bottom, the timing of three major phases in the diatom communities in the DeepCHALLA sequence (Tanttu, 2021), the lithofacies category of each sediment horizon (colored bar), and the depositional stages (V-I) based on the seismic stratigraphy of Lake Chala, as well as (a) the lake level reconstruction based on the seismic reflection data (Maitituerdi et al., 2022). (b) The BIT index from the DeepCHALLA sequence in light grey with green and pink curves representing the band pass filtered periods reflected by wavelet analysis which are comparable to the periods of precession and obliquity, respectively. (c) Wavelet analysis using morlet function with warm and cold colors reflect high and low values of the power spectrum, respectively. (d) The wavelet spectra resulting from analysis of the full sequence DeepCHALLA sequence, and additionally (e) wavelet spectra from analysis of 180–0 ka only. The red stippled line in panels (d) and (e) represents the 95% confidence interval.

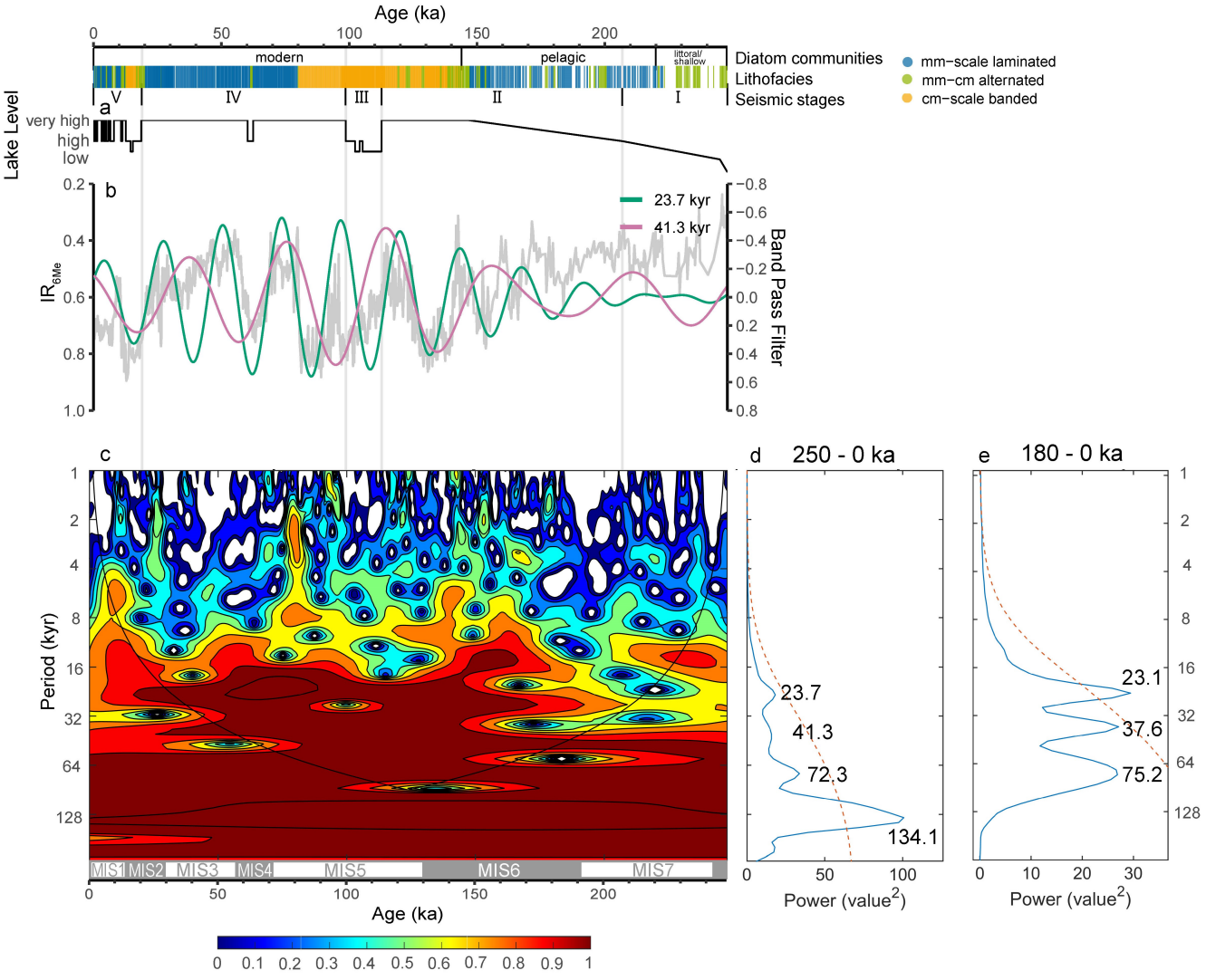

Figure S10. As described for Fig. S9 but for the ratio of the between 6-Me and 5-Me brGDGTs (IR_{6Me}).

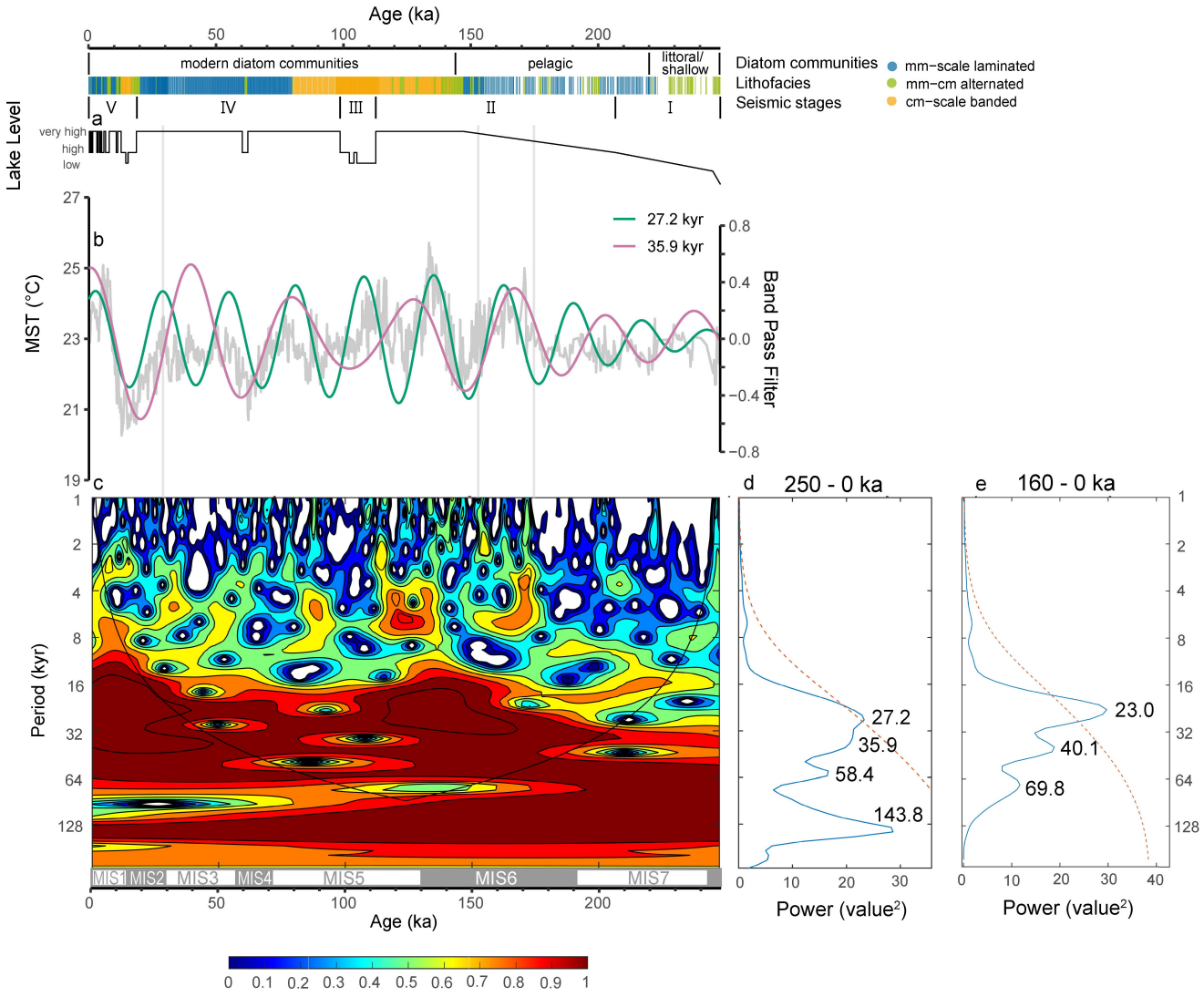

Figure S11. As described for Fig. S9 but for Mean Summer Temperature (MST), reconstructed based on a calibration using brGDGT abundances in globally distributed lake sediments (Pearson et al., 2011), and where panel (e) reflects the period 160 - 0 ka.